Mediterranean Archaeology and Archaeometry, Vol. 18, No 3, (2018), pp. 103-120

DOI: 10.5281/zenodo.1461623

FUNGAL BIODETERIORATION OF ARTIFICIAL AGED LINEN TEXTILE: EVALUATION BY MICROSCOPIC, SPECTROSCOPIC AND VISCOMETRIC METHODS

Abdelrahman Elamin[1*], Kosuke Takatori[2], Yasunori Matsuda[3], Masahiko Tsukada[4] and Fumiyoshi Kirino[4]

[1] Graduate School of Conservation and Cultural Properties, Tokyo University of the Arts, Ueno-koen, Taito-ku, Tokyo 110-8714, Japan; Conservation Center of the Grand Egyptian Museum (GEM), Giza, Egypt
[2] Center for Fungal Consultation, Yukigaya-Ohtsuka, Ohta-ku, Tokyo 145-0067, Japan
[3] Toyo Institute of Art & Design, Tomihisa-cho, Shinjuku-ku, Tokyo 162-0067, Japan
[4] Graduate School of Conservation and Cultural Properties, Tokyo University of the Arts, Ueno-koen, Taito-ku, Tokyo 110-8714, Japan

Received: 17/07/2018
Accepted: 02/10/2018
[*]Corresponding author: Abdelrahman Elamin (elamin_555@hotmail.com)

ABSTRACT

The majority of textiles in ancient Egypt are made from the flax plant (*Linum usitatissimum*). Cloth made from flax is defined as linen. It was predominantly used for wrapping Egyptian mummies, an important stage in the mummification process. Fungal deterioration of ancient linen textiles is one of the most serious problems in the museum field. The relationship between ancient linen objects from different periods and their susceptibility to fungal deterioration is a critical issue in collections management in museums. In the present study, four groups of samples were prepared with different aging conditions. These samples were inoculated with the spores of four species of fungi that possess cellulolytic activity (*Alternaria alternata*, *Chaetomium globosum*, *Aspergillus flavus* and *Penicillium oxalicum*) and incubated for one month. The control and deteriorated samples of each group were evaluated by using visual assessment, light microscope (LM), scanning electron microscope (SEM), X-ray diffraction (XRD), viscometer method and Fourier transform infrared (FTIR) spectroscopy. It was concluded that fungal mechanisms of deterioration occurred in the form of hydrolysis, oxidation, depolymerization and recrystallization processes. Decreasing the influence of fungi by increasing the aging of linen textile samples was demonstrated. *A. alternata* and *C. globosum* showed the highest enzymatic activity in the samples from all groups as compared with other species.

KEYWORDS: Aged linen textile, Fungi, Fibrillar morphology, Crystallinity, Oxidation, Cellulose chain breaks.

1. INTRODUCTION

Textiles are an important reference source for cultural studies, since they represent a significant aspect of craft production that correlates directly with people and their culture. The majority of ancient Egyptian textiles are of linen, which was made from flax. Egyptian mummies were permanently wrapped in linen (Abdel-Maksoud and El-Amin, 2011) because it was considered a symbol of light and purity as well as a demonstration of wealth (El-Gaoudy et al., 2011).

The modes of cellulose degradation include chemical (acid hydrolysis, enzymatic hydrolysis, alkaline degradation and oxidative degradation), thermal (different temperature levels) and radiation (exposure to UV/visible radiation). In nearly all modes of cellulose degradation, cellulose macromolecular structure (crystallinity or fibrillar morphology) plays a decisive role in determining the rate and also often the course of a degradation process. A high macromolecular order of the polymer chain generally impedes degradation (Area and Cheradame, 2011). A deteriorative reaction of textile fibers may occur homogeneously throughout a fiber or may proceed heterogeneously, such as beginning on the fiber surface and subsequently proceeding inward. In addition, aging may occur with morphological specificity, such as in only noncrystalline regions of a fiber. An aging reaction may alter the molecular weight, crystallinity or orientation of the fibers. The gross size or shape of fibers may change during aging. Finally, the chemical composition of fibers may be altered, such as changing the chemical structure of the polymer (Bresee, 1986).

Most of organic archeological objects show the highest microbial growth (bacteria and fungi) (Elserogy et al., 2016). Biodeterioration phenomena represent complex, natural, physical and chemical spoilage processes in textile objects, the majority of which are currently considered cultural heritage, and are caused by the growth of very different organisms (Pinzari et al., 2006). The deterioration of textile objects displayed in exhibition halls or storage facilities and their spoilage by fungi is nowadays a significant problem for cultural heritage conservators (Sterflinger, 2010; Grbić et al., 2013). Textile fibers are susceptible to biocorrosion due to the content of chemical individuals, which are a nutrient for microorganisms. Linen textile decomposes in enzymatic hydrolysis as a result of several fungi (*Alternaria, Chaetomium*, *Myrothecium*, *Neurospora*, *Penicillium*, *Scopulariopsis*, *Aspergillus*, *Stachybotrys* and *Stemphylium* (Cybulska et al., 2008). However, this is not the only problem. The metabolisms of fungi produce acidic wastes, which contribute to cellulose degradation (Area and Cheradame, 2011). The mycelia and spores of fungi cover the surface of some textiles' fibers making them opaque, pitted and rough (Abdel-Kareem et al., 2010). Fungi also have the ability to form hyphal networks, which deeply penetrate materials (Sterflinger and Pinzari, 2012). Elamin et al. (2018) demonstrated that change of the morphological structure, increasing of the carbonyl content and decreasing of the crystallinity are the characteristic aspects of biodeteriorated ancient linen textile.

The susceptibility of aged textiles to fungal deterioration is a critical issue in the field of collections management in museums. The results from several studies raise questions concerning the relationship between the aging and fungal deterioration of textiles. Kavkler and Demšar (2012) stated that the structural changes in textiles caused by fungi begin earlier in the non-aged samples; whereas, in the artificially aged samples, the processes begin later on, but more intensive in the long run. Kavkler et al. (2015b) demonstrated that artificial aging caused structural changes, which "opened" the structure of the cellulose and made it more accessible to fungal attack. By contrast, Łojewska et al. (2017) mention that the amorphous regions disappear in the cellulosic material through aging, and are crystallized to a high degree. Thus the diffusion routes for water and oxygen are cut off, and hydrolysis and oxidation cease. Cowling (1958) mentioned that the resistance of celluloses to enzymatic breakdown is a function of their degree of crystallinity. Palme (2015) states that high-ordered chains are so tightly packed that no water can penetrate between them; whereas, the more open structure in the amorphous cellulose allows more water to interact with the cellulose chains. The present study aims to evaluate clearly this argute point by using a series of measurements for the purpose of following the behavior of several fungal strains upon linen textiles, which are aged under different conditions.

2. MATERIALS AND METHODS

2.1. Linen fabric

The modern, unbleached, plain, flax linen fabric (Table 1) was kindly supplied by Linnet Co., Ltd. for use in the experiments. The protocol of the experimental samples' preparation and the analytical study is illustrated schematically in Appendix.

Table 1. The constructional parameters of the flax linen fabric used in the experiments

Flax linen fabric	Thread/cm		Weight (g)/m²	Thickness (mm)
	Warp	Weft		
	14	13	500	0.6

2.2. Fungal strains

Fungal strains of *Alternaria alternata* (AB.033E), *Chaetomium globosum* (AB.034E), *Aspergillus flavus*

(AB.036E) and *Penicillium oxalicum* (AB.041E), which are stored at the Center of Fungal Consultation, Japan (CFCJ), were chosen for use in this study. These strains were isolated previously from ancient Egyptian linen textiles.

2.3. Preparation of the linen samples

2.3.1. Washing of the samples

For the purpose of removing water-soluble manufacturing materials from the linen fabrics, linen samples were cut into the dimensions of 3×3 cm^2, and immersed for 1⁄2 h in distilled water at 50°C (using a liquid to fabric ratio of approximately 100:1). The samples were agitated by occasionally stirring them with a glass rod. They were rinsed three times in fresh amounts of warm (50°C), distilled water and dried in an oven at 50°C overnight (ASTM- D 629, 2000).

In order to remove the water-insoluble manufacturing materials, all samples were treated with methanol: benzene (1:1) for 24 hrs. Then, samples were dried under a fume hood for 2 hrs (Gassan and Bledzki, 2001).

2.3.2. The groups of linen samples

After the washing process, the samples were divided into four groups: (group UA) un-aged samples, (group 120) and (group 240) samples for heat aging and (group 240U) samples for aging by both heat and UV irradiation. Each group contained 50 samples: 40 samples for fungal deterioration and 10 samples as control.

2.3.3. The artificial aging of the samples

Washed linen samples were subjected to accelerated aging through heat treatment at 150°C in oven model DKN 402 (Yamato Scientific Co., LTD): 120 hrs (group 120), 240 hrs (group 240) and 240 hrs in addition to 96 hrs of UV light (group 240U) at UV Fade Meter U48 (Suga Test Instruments Co., Ltd.).

2.3.4. Fungal deterioration of the linen samples

Spores from the stored fungal strains were germinated at 25°C on potato dextrose agar (PDA). The spores of each strain were collected from culture on agar plates after seven days of incubation. The spore suspension concentrations of *A. alternata*, *C. globosum*, *A. flavus* and *P. oxalicum* were estimated using a Neubauer Chamber Cell Counting to 10^6 cfu/ml. Czapek-Dox Agar medium was prepared by removing the sucrose from its contents, which serves as the sole source of carbon. On each petri dish containing the modified Czapek-Dox Agar medium, 100 µl of the spore suspension from each strain (10^6 cfu/ml) were spread. Eighty petri dishes were used in this study. The spores of the same strain inoculated every 20 petri dishes. The ten sterilized linen samples of each group were put on the surface of the modified Czapek-Dox Agar medium inoculated by the same strain (two samples in each dish). The petri dishes were incubated at 28 ± 2°C and relative humidity at 80 ± 5% for one month. After incubation, the samples were rinsed in ethanol/water solution (70%/30% volume fraction), and then dried at room temperature.

2.4. Investigation methods

2.4.1. Visual assessment by digital camera

In order to show the features of fungal growth on the surface of examined samples from tested groups, a high resolution digital camera (Kodak EasyShare M1033, 10 MP with 3xOptical Zoom) was used to create realistic, photographic documentation of the fungal growth. Visual observation was used to follow the changes in the rate of the mycelial growth of fungi, depending on the aging condition of each group.

2.4.2. Investigation of the morphological structure by light microscope (LM) and scanning electron microscope (SEM)

Fibers from the fungal deteriorated samples of the four tested groups were fixed on a microscope slide with lactophenol, and observed under the light microscope (Olympus BX51) to determine their morphophysiological changes by comparison with control samples of un-aged and aged groups.

Scanning electron microscopy (SEM) was performed on a Hitachi S-2460N SEM microscope, using a high vacuum. The images were obtained in secondary electron image mode. The voltage was 25 kV, while the working distance was 23 mm. The SEM was used to observe the surface morphology of the tested samples (control and fungal deteriorated). The samples' surfaces were sputter-coated with gold (SC-701AT; quick Auto coater, Sanyu Electron Inc, Tokyo, Japan).

2.4.3. Determination of the crystallinity index (*CrI*) by X-ray Diffraction (XRD)

The crystallinity index (*CrI*) of the tested samples was determined by X-ray diffraction analysis (XRD). The analysis of control and deteriorated linen textile samples were carried out on X-ray diffractometer (Rigaku Ultima III). The samples were analyzed using CuKa radiation (λ=1.54Å) at a power of 40 KV and current of 50 mA with 2θ in the range of 10-40 at scan rate (1˚min^{-1}). The *CrI* for linen samples was computed according to the Segal et al. relationship

(Abdelkreem and El-Nagar, 2005) by using the empirical equation (eq. 1).

$$CrI = \frac{I_{002}-I_{am}}{I_{002}} \times 100 \quad (1)$$

Where *CrI* expresses the relative degree of crystallinity, I_{002} is the maximum intensity of the (002) lattice diffraction at 2θ ~ 22˚, and I_{am} is the intensity of diffraction at 2θ ~18˚. I_{002} represents both crystalline and amorphous regions, while I_{am} represents only the amorphous part (Xu et al., 2015). The collected data (Fig. 4; Appendix C) is an average of three measured replications of each sample.

2.4.4. Measurement of the degree of polymerization (*DP*) by viscometer method

The viscosity average degree of polymerization (DP_v) of control and deteriorated samples were determined. Using 0.3 g of each sample, they were reduced for 1 hour with 30 ml of borane tert-butylamine complex solution (0.2 mol/L). Moreover, 4 mg (0.2 g/L) of each reduced sample were dissolved in cupriethylenediamine solution (CED) (GFS Chemicals). The *DP* was calculated from the results of viscosity measurements in CED solution with a Cannon-Fenske viscometer (Sibata, No. 100; Sibata Scientific Technology Ltd.) at 25.0 ± 0.1˚C from a measurement of 1 concentrated solution and calculated by using (eq. 2) (Gassan and Bledzki, 2001; Khan and Alam, 2012).

$$DP = \frac{\eta_{sp}}{1+0.28\,\eta_{sp}} \times \frac{200}{c} \quad (2)$$

$$\text{with :} \quad \eta_{sp} = \frac{t}{t_0} - 1$$

where η_{sp} is the specific viscosity, c (g/100 mL) is the concentration of linen fibers, t (s) is the flow of the fiber-CED solution and t_0 (s) is the time of flow of the CED solution alone. The given *DP* values in this study are average values based on two samples.

2.4.5. Calculation of the number of cellulose chain breaks

In order to calculate the average number of cellulose chain breaks, it is necessary to change the viscosity average degree of polymerization (DP_v) mentioned above into the number-average degree of polymerization (DP_n). In the case of cellulose, DP_n is generally considered to be 1.96 times the DP_v. Since the DP_n means how many mols of glucose are contained per 1 g of cellulose on average, the difference of this combined concentration before and after degradation serves as the number of cellulose chain breaks Δ*C* (Chains, μmol/g) (eq. 3) (Lee and Inaba, 2013).

$$\Delta C\,(\text{Chains}) = \frac{1.96}{162}\left(\frac{1}{DP_{vt}} - \frac{1}{DP_{v0}}\right) \times 10^6 \quad (3)$$

Where DP_{vt} is the viscosity average degree of polymerization after accelerated aging and/or fungal deterioration, and DP_{v0} is the viscosity average degree of polymerization before accelerated aging and/or fungal deterioration.

2.4.6. Measurement of the degree of cellulose oxidation

In order to determine the total oxidation of each sample, its degree of oxidation was measured by viscometry. Samples were dissolved, without reducing them, in CED solution (0.5 mol/L) and were heated at 60˚C for 1 hour. The viscosity was measured by the same method mentioned above (25.0 ± 0.1˚C). The degree of oxidation was calculated from the difference with the degree of polymerization of the reduced sample used in eq. 3. If the cellulose molecules were further oxidized, a lower intrinsic viscosity will be determined (Lee and Inaba, 2013).

2.4.7. Determination of the cellulose oxidation by Fourier Transform Infrared Spectroscopy (FTIR)

FTIR spectra of the control aged samples and the fungal deteriorated samples of the four tested groups were recorded by using a Thermo Scientific Nicolet iZ10 FTIR spectrometer in order to determine the oxidation occurring on the surface, based on the effect of accelerated aging and fungal deterioration. The samples were analyzed by the FTIR-ATR method on the diamond crystal in the range between 1400-650 cm^{-1}. Each spectrum is an average of 64 scans, and scanned at a resolution of 4 cm^{-1}. Three different spots from each of the two samples' surfaces (upper and lower) were measured by FTIR-ATR. The upper sample's surface was in contact with the air of the incubation environment, and where the fungal growth happened; whereas, the lower sample's surface was in contact with the modified Czapek-Dox Agar medium. All of the collected spectra were normalized to the maximum peak (1023 cm^{-1}). The averages of the CO band absorption values at the region around 1628 cm^{-1} were calculated, and standard deviations of the collected values were computed.

3. RESULTS AND DISCUSSIONS

3.1. Visual assessment by digital camera

The result of visual assessment of the mycelial growth of fungi based on the samples from the four tested groups after one month of incubation showed different rates of growth depending on both: (1) the condition of aging and (2) the strain of fungi (Fig. 1). Though the detected, abundant mycelial growth of *A. alternata* and *C. globosum* occurred with un-aged

samples (group UA), *A. flavus* and *P. oxalicum* showed low growth based on the samples from the same group. The rate of mycelial growth decreased gradually with the samples deteriorated by *A. alternata* and *C. globosum*, and significantly with the samples deteriorated by *A. flavus* and *P. oxalicum* due to the increase in heat treatment of the linen samples (groups 120 and 240). The fungal growth of all tested fungi exhibited a small increase in samples aged with UV irradiation with heat aging (group 240U) as compared with mycelial growth of the samples from group 240. The mycelia of the *A. alternata* and *C. globosum* respectively exhibited penetration to the lower surface of tested samples. This penetration decreased with high aged samples. *A. flavus* and *P. oxalicum* showed only surface growth in the samples from all tested groups without visible penetration to the lower surface.

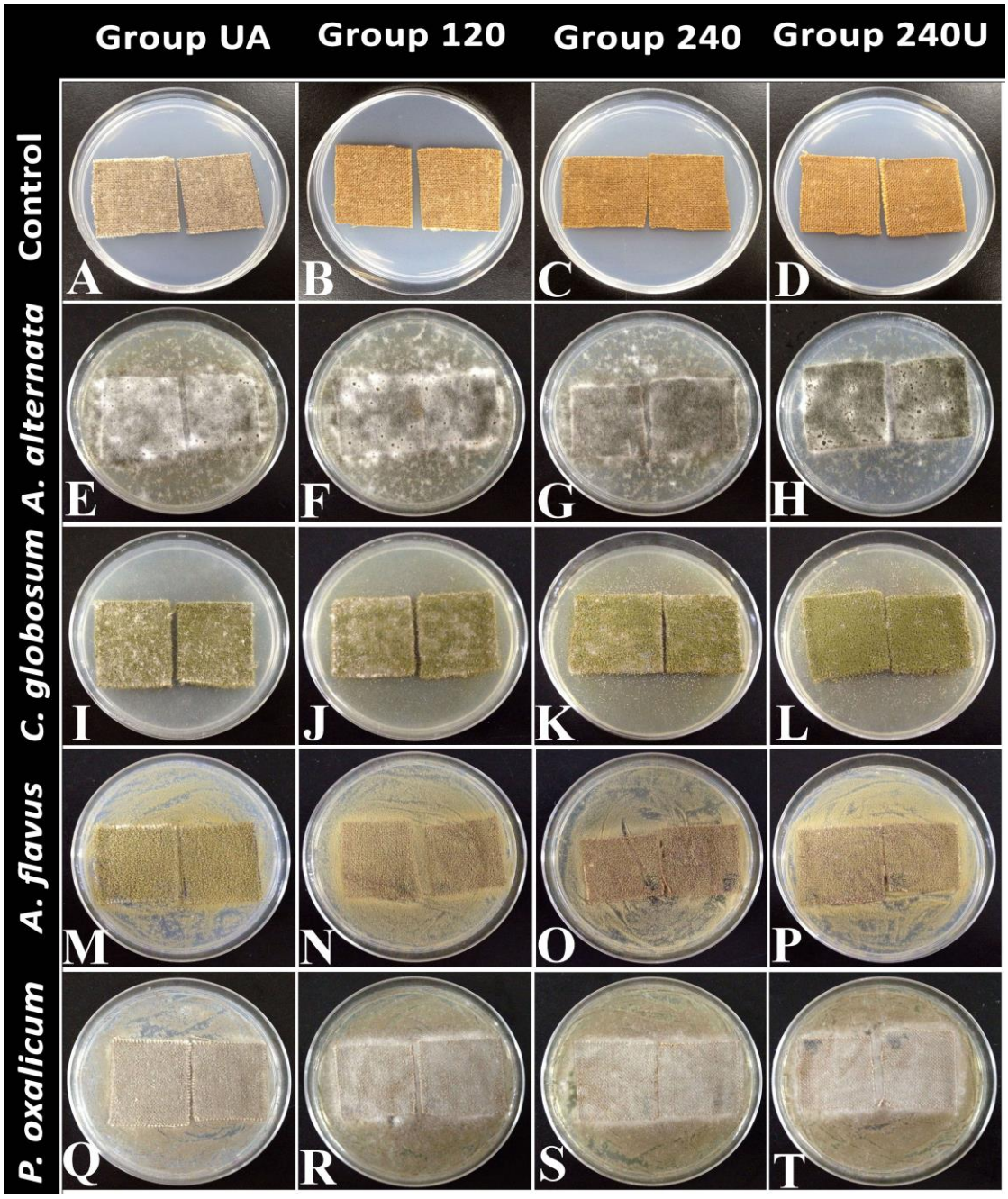

Figure 1. Digital camera photos of the mycelial growth of fungi in samples from the four tested groups. Control samples (A-D): (A) group UA, (B) group 120, (C) group 240 and (D) group 240U. Samples (E-H) deteriorated by A. alternata: (E) group UA, (F) group 120, (G) group 240 and (H) group 240U. Samples (I-L) deteriorated by C. globosum: (I) group UA, (J) group 120, (K) group 240 and (L) group 240U. Samples (M-P) deteriorated by A. flavus: (M) group UA, (N) group 120, (O) group 240 and (P) group 240U. Samples (Q-T) deteriorated by P. oxalicum: (Q) group UA, (R) group 120, (S) group 240 and (T) group 240U

3.2. Investigation of the morphological structure by light microscope (LM) and scanning electron microscope (SEM)

LM and SEM are sophisticated methods, which enabled us to examine the morphology of fiber and fabric surfaces. Microscopic observations were performed on the control and fungal deteriorated samples, in order to demonstrate the effect of the artificial aging treatment on the ability of tested fungi to cause changes in the samples' morphological structure.

Kavkler et al. (2015a) Hamed and Mansour (2018) demonstrated that the degree and speed of fungal deterioration depend on, a. the chemical and physical properties of the substrate (chemical structure, molecular weight and crystallinity), b. enzymatic activity of the fungus, c. the inoculation time. *A. alternata*, *C. globosum*, *A. flavus* and *Penicillium sp.* were found to possess cellulolytic activity, which enable hydrolysis of cellulose polymer enzymatically (Jahangeer et al., 2005).

Compared with control un-aged samples (Fig. 2A; Fig. 3A), the fibers of the control aged samples showed different forms of damage: a roughened surface in samples from groups 120, 240 and 240U (Fig. 3B, C and D), longitudinal splitting characterized by small scratches in samples from groups 120 and 240 (Fig. 2B and C; Fig. 3B and C) and large slits in samples from group 240U (Fig. 2D; Fig. 3D). Amin (2018) stated that longitudinal splitting is characteristic form of damage which accompanying bad preserved ancient textile. According to Kavkler et al. (2015b), these forms of damage happened because of the breakage of intramolecular bonds between microfibrils.

LM and SEM images of the samples deteriorated by tested fungi exhibited different morphological changes. The un-aged samples (group UA) deteriorated by *A. alternata*, *C. globosum* and *A. flavus* respectively (Fig. 2E, I and M; Fig. 3E, I and M) demonstrated spreaded breaks and slits in their fibers, which seem to be superficial. In contrast, *P. oxalicum* (Fig. 2Q; Fig. 3Q) exhibited a low ability in causing visible breaks with un-aged samples. Swilling the fibers of the group UA samples, which deteriorated by all tested strains, was observed (Fig. 2E, I, M and Q). It may be considered a distinguishing form of damage that was not found with the deteriorated samples of aged groups.

The images of the deteriorated samples from group 120 showed that damage was more intensive than the samples from group UA. Longitudinal splitting characterized by cavities was recorded with the samples deteriorated by *A. alternata* and *C. globosum* (Fig. 2F and J; Fig. 3F and J) respectively. The samples deteriorated by *A. flavus* (Fig. 2N; Fig. 3N) showed an extremely roughened surface without any longitudinal splitting. This may be due to the decrease in its ability to penetrate the fibers of group 120 samples. The samples deteriorated by *P. oxalicum* (Fig. 2R; Fig. 3R) exhibited the same form of damage that appeared with un-aged samples, namely roughness of the sample's surface (Fig. 2Q; Fig. 3Q).

The samples from group 240 (Fig. 2G, K, O and S; Fig. 3G, K, O and S) represented a significant decrease in fungal damages as compared with deteriorated samples from group 120. Small surface changes were found in comparison to the control samples of the same group (Fig. 2C; Fig. 3C).

The deteriorated samples of group 240U (Fig. 2H, L, P and T; Fig. 3H, L, P and T) showed a small increase in damage as compared with the deteriorated samples of group 240, but this stated damage is still significantly lower than what was recorded by the samples of groups UA and 120.

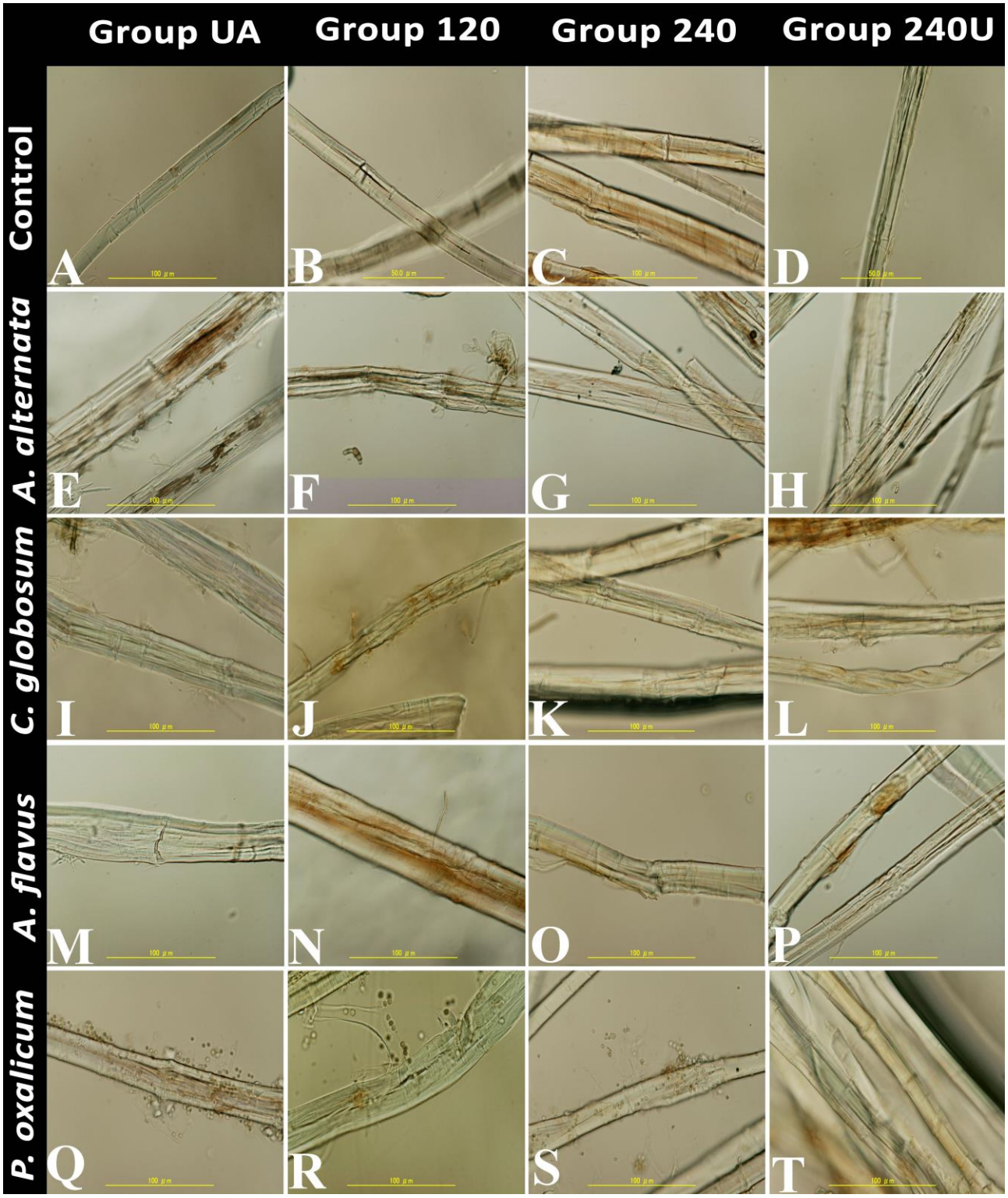

Figure 2. LM images of the samples from the four tested groups. Control samples (A-D): (A) group UA, (B) group 120, (C) group 240 and (D) group 240U. Samples (E-H) deteriorated by A. alternata: (E) group UA, (F) group 120, (G) group 240 and (H) group 240U. Samples (I-L) deteriorated by C. globosum: (I) group UA, (J) group 120, (K) group 240 and (L) group 240U. Samples (M-P) deteriorated by A. flavus: (M) group UA, (N) group 120, (O) group 240 and (P) group 240U. Samples (Q-T) deteriorated by P. oxalicum: (Q) group UA, (R) group 120, (S) group 240 and (T) group 240U

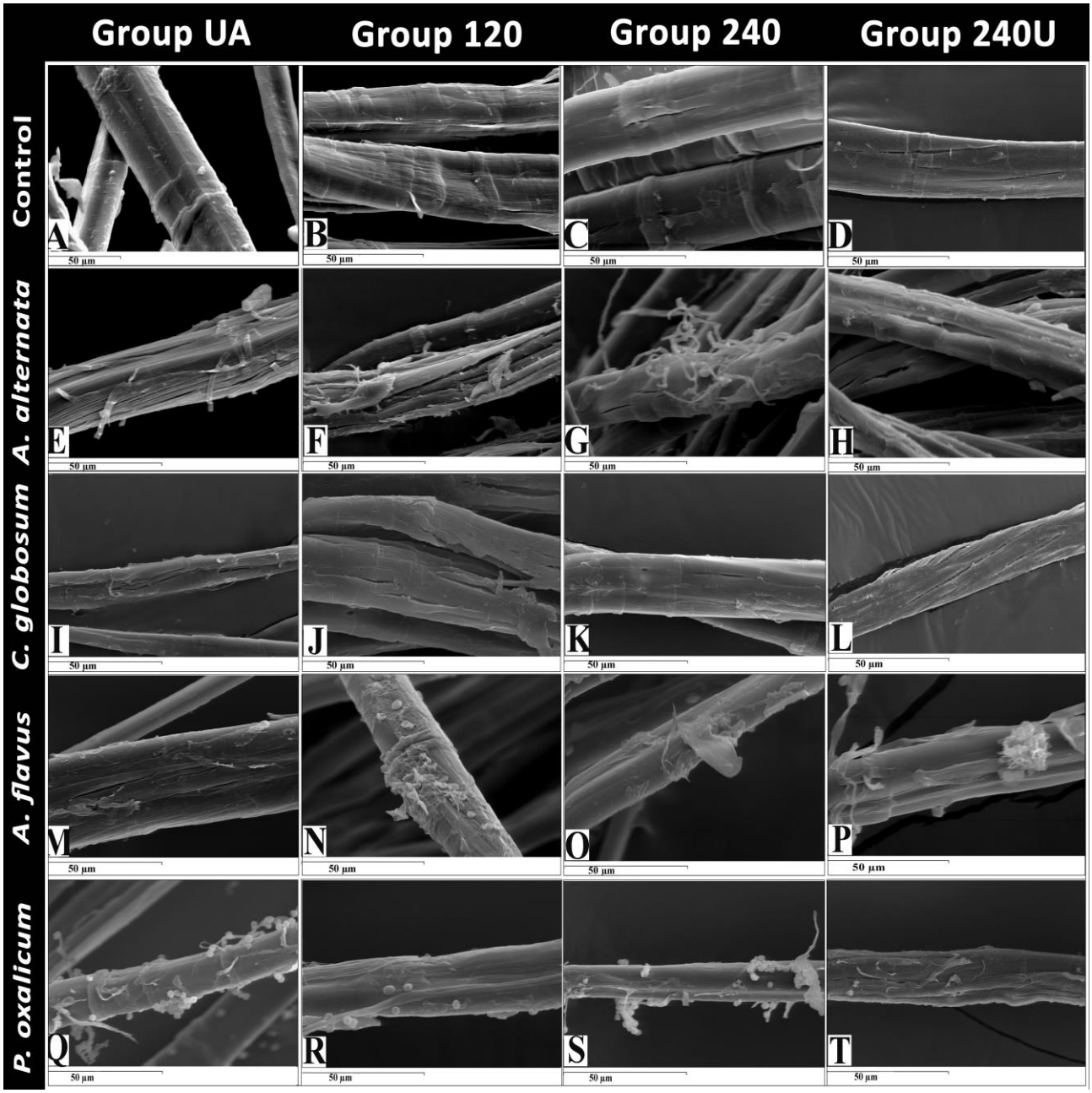

Figure 3. SEM images of the fibers from the four tested groups' samples. Control samples (A-D): (A) group UA, (B) group 120, (C) group 240 and (D) group 240U. Samples (E-H) deteriorated by A. alternata: (E) group UA, (F) group 120, (G) group 240 and (H) group 240U. Samples (I-L) deteriorated by C. globosum: (I) group UA, (J) group 120, (K) group 240 and (L) group 240U. Samples (M-P) deteriorated by A. flavus: (M) group UA, (N) group 120, (O) group 240 and (P) group 240U. Samples (Q-T) deteriorated by P. oxalicum: (Q) group UA, (R) group 120, (S) group 240 and (T) group 240U

3.3. Determination of the crystallinity index (CrI) by X-ray Diffraction (XRD)

XRD was used as a semiquantitative method for determining the *CrI* of examined linen samples (see the XRD diagrams and the collected data from XRD of the tested samples in Appendix B and Appendix C respectively). The collected data demonstrated the role of artificial aging in causing slight increase of the *CrI* of the control samples from groups 120 through 240U in comparison to the control from group UA. The influence of heat aging with cellulosic materials was stated in previous works. Yatagai (1996) mentioned that heat treatments induce cellulose chain scissions, which lead to a higher crystallinity. Gassan and Bledzki (2001) demonstrated that changes in crystallinity of flax textile due to the thermal exposure are usually only slight. The mechanism of cellulose crystallization by heat aging was also discussed by Gassan and Bledzki (2001), who

stated that the crystallization may result from an increase in the size of preexisting crystallites by, for example, realignment of cellulose chains on the crystallite surface or at their ends. It is also possible that the crystallization occurs through the formation of completely new crystallites within the amorphous areas.

Based on the previously mentioned fungal cellulolytic enzymes that easily penetrate from the cellulose amorphous region degrading the cellulose structure, the samples from group UA deteriorated by *A. alternata* exhibited a noticeable decrease in the *CrI* as compared with the control (Fig. 4). A slight decrease was found with the un-aged samples deteriorated by *C. globosum*, *A. flavus* and *P. oxalicum* respectively. This means that the enzymes of tested fungi not only affected the amorphous region of the deteriorated samples from group UA but the crystalline region was also affected.

The results showed that the fungal enzymatic activity was decreased in the high crystalline samples as clearly shown by group 240U. This is reflected by the gradual decrease in the gap between the *CrI* percentages of the deteriorated samples in each of the aged groups (Fig. 4). The relationship between crystalline cellulose and damage was discussed in previous works. Gassan and Bledzki (2001) said that crystalline cellulose is the least susceptible to degradation. Cowling (1958) mentioned that the resistance of celluloses to enzymatic breakdown is a function of their degree of crystallinity. This is because the amorphous regions of cellulose are preferentially attacked by the enzymes; whereas, the more crystalline areas are resistant to enzymatic attack (Bertran and Dale, 1985).

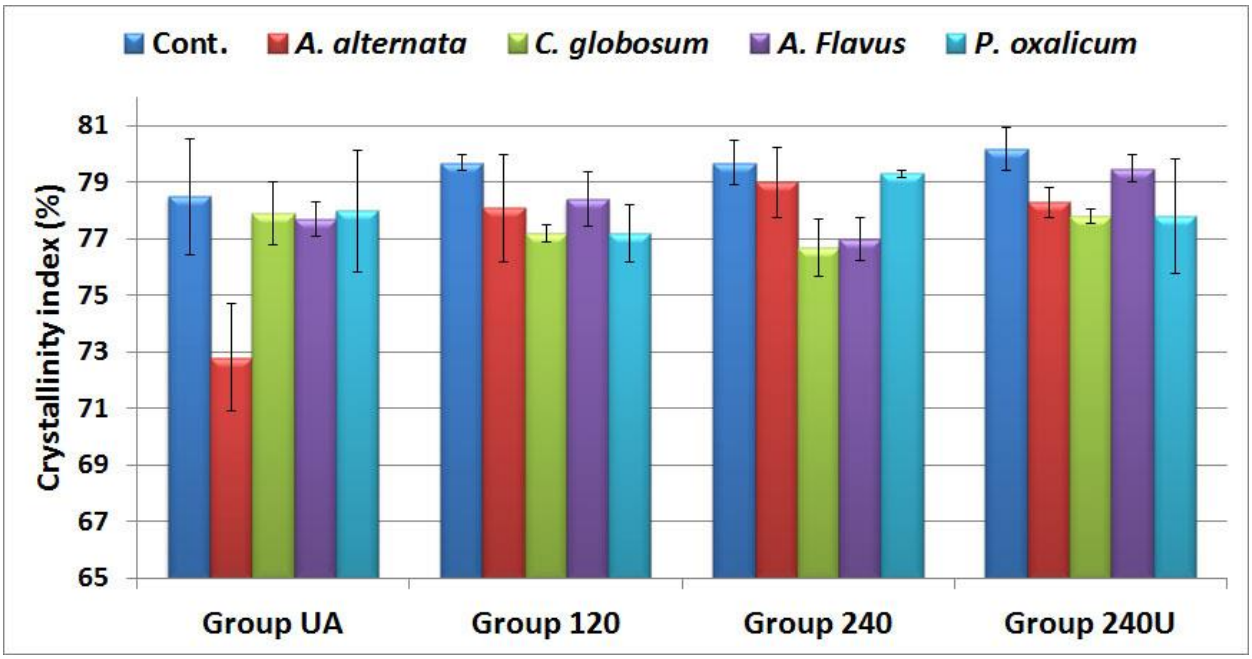

Figure 4. The percentages of the CrI of the samples from the four tested groups based on XRD

3.4. Measurement of the degree of polymerization (DP)

The decrease in the *DP* is a characteristic aspect of cellulose degradation, which is considered the essential degradation mechanism in cellulose (Area and Cheradam, 2011). The present study involved the determination of the *DP* of the control and deteriorated linen samples from the four tested groups (Fig. 5). The aim was to discover the linkage between the decrease in the rate of the *DP* of the fungal deteriorated samples and the aging degree of these samples.

Generally, all of the control aged and deteriorated samples exhibited a decrease in their DP. The dramatic decrease in the DP value of the control aged sample from group 120 was recorded. At Groups 240 and 240U, the control samples moves into the "zero degradation rate" stage and its DP has approached the leveling off degree of polymerization (LODP) indicating the deceleration of the degradation process.

Concerning the difference in *DP* values depending on the influence of the fungal species, the results showed significant gaps between the *DP* values of the samples from each group (especially group UA) deteriorated by tested fungi (*A. alternata*, *C. globosum*, *A. flavus* and *P. oxalicum*). Samples deteriorated by *A. alternata* and *C. globosum* showed a higher decrease in its *DP* values as compared with samples deteriorated by *A. flavus and P. oxalicum*. The resistance of groups 240 and 240U to the depolymerization was clearly recorded.

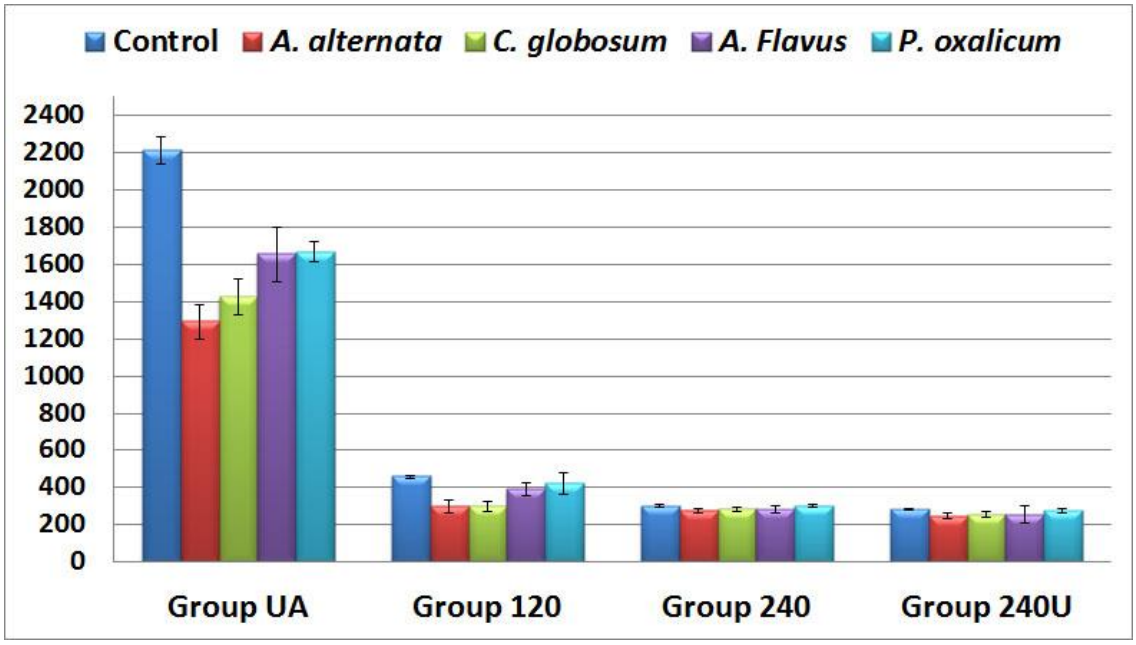

Figure 5. DP of the samples from the four tested groups

3.5. The relationship between the number of cellulose chain breaks and the degree of oxidation

The degrees of oxidation of the samples from the four tested groups were determined by the measurement of the degree of cellulose polymerization, as one indices of how much oxidation had taken place in the cellulose. Then, the degree of oxidation was compared to the number of cellulose chain breaks that occurred through the effect of artificial aging and fungal deterioration.

Although there were some variations, it can be stated that the more the number of cellulose chain breaks increased that the more cellulose oxidation tended to increase. As shown with the control samples (Fig. 6), the increase in the number of cellulose chain breaks proceeded slowly, and the tendency towards oxidation was limited in the high aged samples (controls of groups 240 and 240U). The fungal deteriorated samples of groups 240 and 240U exhibited limited hydrolysis and oxidation caused by the effect of tested fungi (Fig. 7); whereas, the samples from group 120 noticeably showed an increase in the number of cellulose chain breaks and degree of oxidation as compared with the deteriorated samples of other groups.

Concerning fungal strains, *A. alternata* and *C. globosum*, they showed higher enzymatic hydrolysis activity than *A. flavus* and *P. oxalicum*.

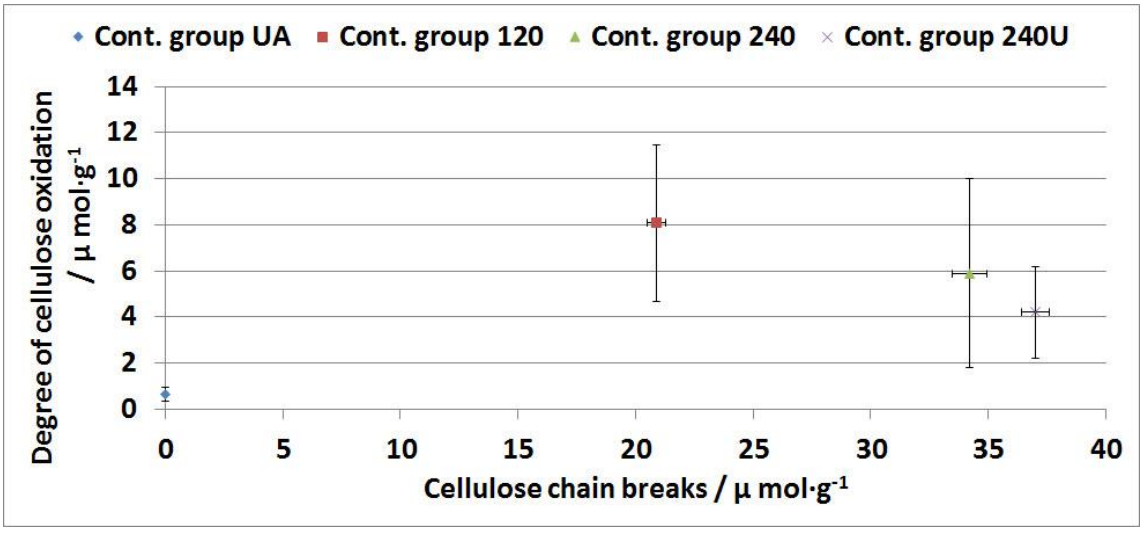

Figure 6. Relationship between the number of cellulose chain breaks and the degree of oxidation of the control samples from the four tested groups

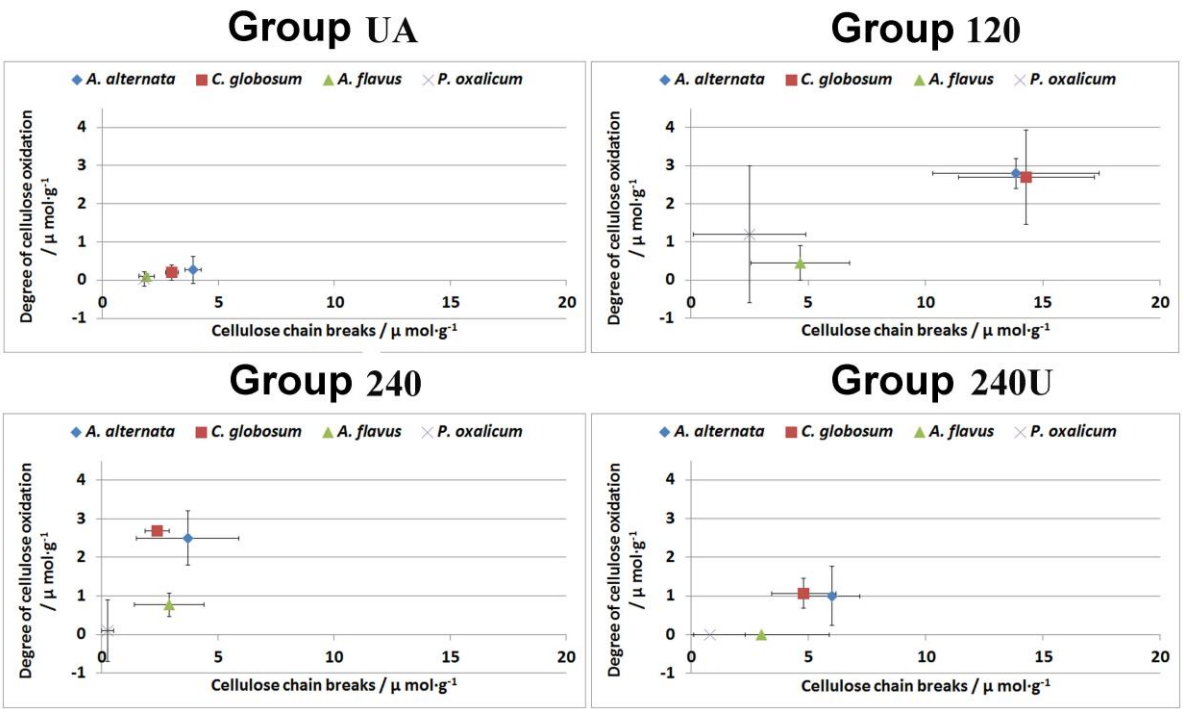

Figure 7. Relationship between the number of cellulose chain breaks and the degree of oxidation of the deteriorated samples from the four tested groups

3.6. Determination of the cellulose oxidation by Fourier Transform Infrared Spectroscopy (FTIR)

The control and deteriorated samples from the four tested groups were analyzed by FTIR-ATR (see FTIR-ATR spectra of the upper and lower surfaces of the samples from the four tested groups in Appendix D). FTIR provides information about cellulose functional groups. The extent of the structural changes of textile samples in vitro depended on: (1) the artificial aging, (2) the infection with specific fungal species and (3) the incubation time (Kavkler et al., 2015b). Fungal enzymatic hydrolysis of textile fibers proceeds heterogeneously, beginning on the fiber's surface where fungal mycelial growth is found and subsequently proceeding inward. Thus, the two surfaces of each sample were measured for the purpose of evaluating the ability of each tested fungal strain to damage and penetrate the fibers of un-aged and aged samples.

Since cellulose-based materials' vibrational spectrum is on the complex side, a good candidate for tracing the changes in cellulosic materials caused by hydrolysis and oxidation are carbonyl groups (–COOH, –CHO and –CO), which occur on the broken ends of macromolecular chains (Łojewska et al., 2006; Kavkler and Demšar, 2012). According to Abdel-Maksoud and El-Amin (2013) the region around 1750-1600 cm^{-1} was proved to be the most convenient for monitoring cellulose degradation. The general common trend for all the control aged samples is the evolution of the broad bands with maxima at around 1730 and 1628 cm^{-1} (Fig. 8). The collected spectra showed that the broad band at region ~1628 cm^{-1} increased with the fungal deteriorated samples of each group in comparison to the control (Table 2 and Fig. 8). No significant increase in the band at 1730 cm^{-1} was noticed with the fungal deteriorated samples from all tested groups. According to Ferrero et al. (1998), the increase in the absorbency of the band intensity at region 1730 cm^{-1} appears to be highly influenced by thermal treatment.

It was noticed that the influence of the oxidation process caused by fungi was at its peak based on the samples from group UA. As shown in Table 2 and Figure 8, the influence of fungi decreased gradually with the increase in the aging condition of the samples from aged groups (groups 120, 240 and 240U). The difference between the intensities' height of the bands at region ~1628 cm^{-1} of the samples from groups UA and 120 deteriorated by *A. alternata*, *C. globosum*, *A. flavus* and *P. oxalicum* was clear and characterized by the effect of each strain; whereas, this difference was so close to the spectra of deteriorated samples of groups 240U and 240 respectively. This means that the ability of the fungi to cause damage was limited with the high aged samples. Comparing the intensities' bands at 1628 cm^{-1} of the upper (highly deteriorated) and lower surfaces of tested groups' samples, *C. globosum* exhibited high and stable oxidative ability to the cellulose components of the upper surfaces of samples of the aged groups as compared with other strains (Fig. 8A). In

contrast, *A. alternata* exhibited rapid growth and a higher ability to penetrate samples in the lower surfaces (Fig. 8B). Also, the analysis of the lower surfaces of deteriorated samples shows less damage than the upper surfaces.

Table 2. FTIR data from the upper and lower surfaces of each sample from the four tested groups (SD refers to standard deviation)

Group	Sample	Sample's upper surface		Sample's lower surface	
		Absorbency at 1628 cm^{-1}		Absorbency at 1628 cm^{-1}	
		Value	SD	Value	SD
UA	**Cont.**	0.131	0.001	0.130	0.005
	A. alternata	0.340	0.020	0.271	0.03
	C. globosum	0.213	0.010	0.200	0.029
	A. flavus	0.164	0.020	0.136	0.003
	P. oxalicum	0.141	0.010	0.135	0.020
120	**Cont.**	0.133	0.003	0.133	0.001
	A. alternata	0.220	0.030	0.189	0.006
	C. globosum	0.174	0.001	0.153	0.002
	A. flavus	0.145	0.007	0.133	0.001
	P. oxalicum	0.140	0.005	0.138	0.006
240	**Cont.**	0.136	0.001	0.136	0.0004
	A. alternata	0.163	0.013	0.141	0.005
	C. globosum	0.220	0.006	0.154	0.004
	A. flavus	0.147	0.002	0.142	0.005
	P. oxalicum	0.139	0.006	0.138	0.002
240U	**Cont.**	0.138	0.0003	0.138	0.0001
	A. alternata	0.179	0.010	0.172	0.001
	C. globosum	0.231	0.008	0.144	0.004
	A. flavus	0.138	0.001	0.137	0.003
	P. oxalicum	0.135	0.002	0.132	0.004

Though the collected results from all measurements show the same trend with the samples from the aged groups, the group UA samples gave confusing results. It showed: (1) noticeable damage in its fibers' morphological structure, (2) a low number of cellulose chain breaks and a low degree of oxidation as stated by the viscometer method and (3) high content of carbonyl groups as stated by normalized spectra of FTIR-ATR. To elucidate this confusion, it should be mentioned that cellulase enzymes can attack the amorphous regions of cellulose chains; and thus making it is easier to separate the cellulose structures by the mechanical damage caused by the mycelia of fungi, as demonstrated by the SEM images of the deteriorated un-aged samples. The amorphous region is easily accessible to enzymes, and can be degraded due to hydrolysis and oxidation reactions. In contrast, the crystalline region (ordered structure) is difficult to attack by enzymes. Studies with pure cellulose have shown that the rate of hydrolysis of the amorphous cellulose is five to thirty times higher than that of crystalline cellulose, so that the CO contents in crystalline and amorphous regions will be different (Rao, 2009; Yang, 2011). Henriksson et al. (2007) stated that enzyme treatment was found to facilitate disintegration of fresh cellulose fiber, while the molecular weight and length of cellulose nanofibers were both well preserved. Ciolacu et al. (2011) demonstrated that viscosity measurements have shown that a slight depolymerization occurs in cellulose samples during the dissolution of the amorphous region from its structure. Based on these previous results, the difference between the decrease in the degree of oxidation, which is measured by viscometer method, and the increase in the measured oxidation by FTIR-ATR in the current study can be attributed to the difference between each of the two methods in measuring the changes occurring in the amorphous region. Therefore, one can say that the presence of the amorphous region in un-aged samples responds differently to fungal deterioration as compared with the aging samples. This extracted result also agrees with Gao et al. (2014), who mentioned that the dried cellulosic samples have a completely different macromolecular structure and substrate reactivity from fresh cellulosic samples.

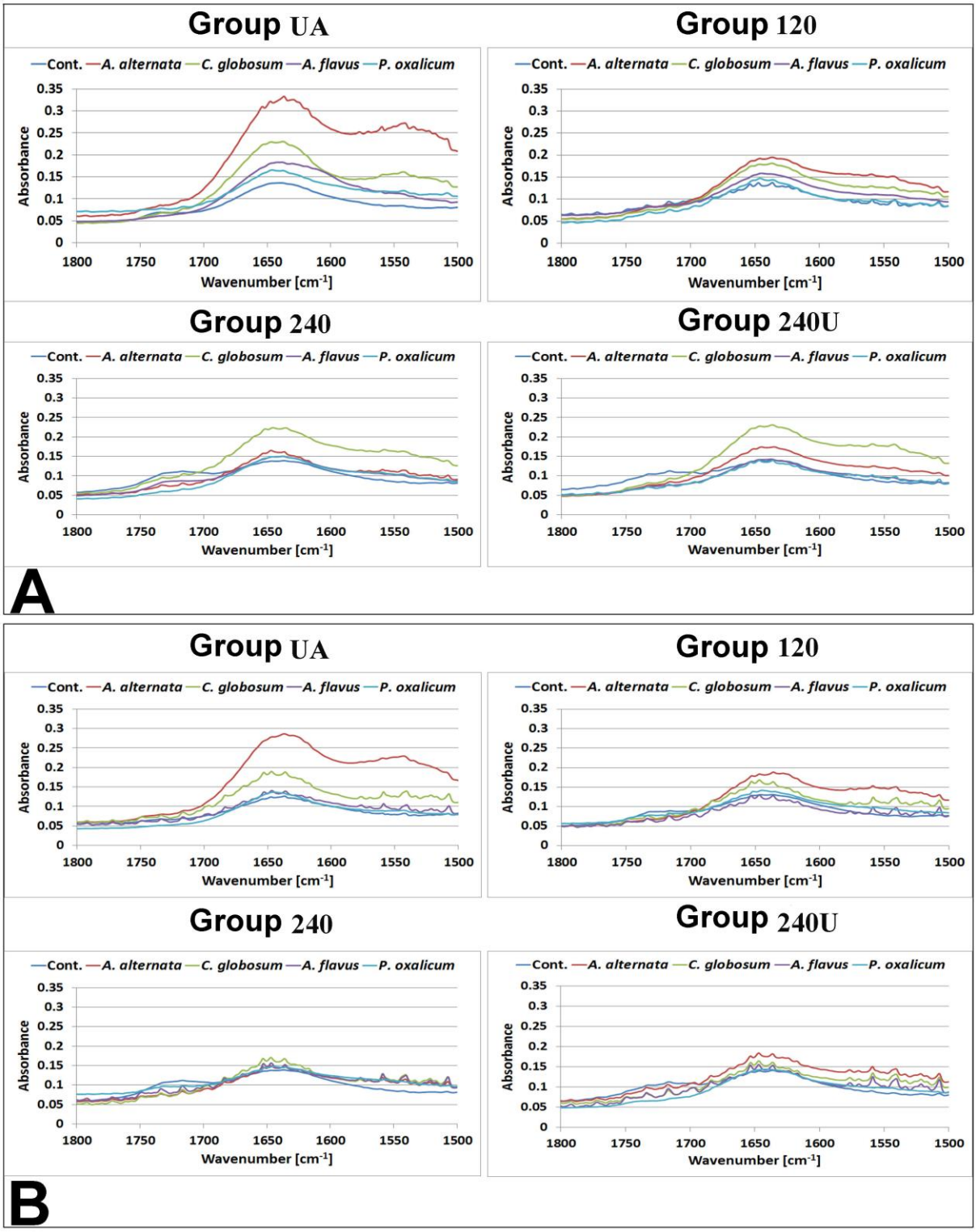

Figure 8. FTIR spectra of the CO region of the samples from the four tested groups: (A) Upper surface and (B) Lower surface.

4. CONCLUSIONS

The physicochemical properties of flax linen fibers and the species of fungi are the most important factors affecting the fungal deterioration of linen fibers. Morphological changes, oxidation, hydrolysis, depolymerization and recrystallization are the characteristic deteriorative processes accompanying the artificial aging (thermal and UV irradiation) and fungal deterioration. The deterioration mechanism of fungi is a process highly linked to the aging condition of linen textiles, which decreases with the high aged samples. Longitudinal creases were observed by microscopic investigation as a significant aspect

of fungal deterioration to the morphological structure of linen fibers.

It was found that the ratio between amorphous and crystalline regions of tested linen samples is the main factor affecting the mechanism of fungal deterioration as follow: fungal mycelium structure and enzymes easily penetrate the amorphous regions, as shown with un-aged samples, facilitating the occurrence of hydrolysis and oxidation of the whole amorphous region with slight damage to the crystalline region. The different measurements showed that the most intensive damage was found in the samples from group 120 (control and deteriorated) as compared with the damage occurring to the samples of other aged groups. It can be stated that a low aging condition (group 120 in the case of the current study) works as an intermediate stage (transitional) from un-aging to high aging; while the amorphous region was degraded, the crystalline region was beginning to rearrange and some breakdown occurred between the intermolecular and intramolecular bond. By this time, the sample's structure is accessible to the mechanisms of fungal deterioration, and high damage happens. Regarding the high aged linen samples (group 240 and 240U), the susceptibility of the groups' samples to fungal attack is totally different from what occurred with group 120 samples. By increasing the samples' crystallinity index, the diffusion routes of enzymes are stopped; and, the hydrolysis and oxidation processes slow down or cease.

The tested fungi exhibited different enzymatic activity as compared with the samples from each of the tested groups. *A. alternata and C. globosum* showed higher enzymatic activity than *A. flavus* and *P. oxalicum* based on the samples from different groups.

ACKNOWLEDGEMENTS

A. Elamin thanks the Ministry of Education, Culture, Sports, Science and Technology (MEXT) of Japan for a scholarship for his Ph.D. The deepest gratitude to Prof. Masamitsu Inaba from Graduate School of Fine Arts, Tokyo University of the Arts for his helps with discussion of results and ideas.

REFERENCES

Abdel-Kareem, O. and Alfaisal, R. (2010) Treatment, conservation and restoration of the Bedouin dyed textiles in the museum of Jordanian heritage, *Mediterranean Archaeology and Archaeomtry*, Vol. 10, No. 1, pp. 25-36.

Abdel-Kreem, O. and El-Nagar, K. (2005) Non-destructive methods to investigate the deterioration extent of Coptic Egyptian textiles, *JTATM*, Vol. 4, No. 4, pp. 1-15.

Abdel-Maksoud, G. and El-Amin, A. (2011) A review on the materials used during the mummification processes in ancient Egypt, *Mediterranean Archaeology and Archaeomtry*, Vol.11, No.2, pp. 129-150.

Abdel-Maksoud, G. and El-Amin, A. (2013) The investigation and conservation of a gazelle mummy from the late period in ancient Egypt, *Mediterranean Archaeology and Archaeomtry*, Vol. 13, No 1, pp. 45-67.

Amin, E. A. (2018) Technical investigation and conservation of a tapestry textile from the Egyptian textile museum, Cairo, *SC*, Vol. 4, No 3, pp. 35-46.

Area, M. Cr. and Cheradame, H. (2011) Paper aging and degradation: recent finding and research methods, *BioResources*, Vol. 6, No. 4, pp. 5307-5337.

ASTM- D 629 (2000) *Standard test methods for quantitative analysis of textiles*, United States.

Bertran, M. S. and Dale, B. E. (1985) Enzymatic hydrolysis and recrystallization behavior of initially amorphous cellulose, *Biotechnol. Bioeng*., Vol. 27, pp. 177-181.

Bresee, R. R. (1986) General effects of ageing on textiles, *JAIC*, Vol. 25, No. 1, pp. 39-48.

Ciolacu, D., Ciolacu, F. and Popa, V. I. (2011) Amorphous cellulose - structure and characterization, *Cell. Chem. Technol*., Vol. 45, No. 1-2, pp. 13-21.

Cowling, E. B (1958) *A review of literature on the enzymatic degradation of cellulose and wood*, Madison, Wis.: U.S. Dept. Of Agriculture, Forest Service, Forest Products Laboratory, on line at http://ir.library.oregonstate.edu/concern/defaults/79408203w

Cybulska, M., Jedraszek-Bomba, A., Kuberski, Sl. and Wrzosek, H. (2008) Methods of chemical and physicochemical analysis in the identification of archaeological and historical textiles, *Fibres Text. East. Eur*., Vol. 16, No. 5, pp. 67-73.

Elamin A., Takatori, K., Matsuda, Y., Tsukada, M. and Kirino, F. (2018) Microbiological, morphological and spectroscopic study on the effect of resinous materials in the preservation of wrapping textiles of mummies, *Mediterranean Archaeology and Archaeomtry*, Vol. 18, No 2, pp. 1-10.

El-Gaoudy, H., Kourkoumelis, N., Varella, E. and Kovala-Demertzi, D. (2011) The effect of thermal aging and color pigments on the Egyptian linen properties evaluated by physicochemical methods, *Appl. Phys. A*, Vol. 105, No. 2, pp. 497–507.

Elserogy, A., Kanan, Gh., Hussein, E. and Abd-Khreis, Sh. (2016) Isolation, characterization and treatment of microbial agents responsible for the deterioration of archaeological objects in three Jordanian museums, *Mediterranean Archaeology and Archaeomtry*, Vol. 16, No 1, pp. 117-126.

Ferrero, F., Testore, F., Malucelli, G. and Tonin, C. (1998) Thermal degradation of linen textile: the effect of aging and cleaning, *J. Text. I.*, Vol. 89, No. 3. https://doi.org/10.1080/00405009808658642. 5/12/2016

Gao, Sh., Chun, Ch., Renneckar, Sc., Bao, J. and Zhang, Y-H. P. (2014) New insights into enzymatic hydrolysis of heterogeneous cellulose by using carbohydrate-binding module 3 containing GFP and carbohydrate-binding module 17 containing CFP, *Biotechnol. Biofuels*, Vol. 7. https://doi.org/10.1186/1754-6834-7-24

Gassan, J. and Bledzki, A. K. (2001) Thermal degradation of flax and jute fibers, *J. Appl. Polym. Sci.*, Vol. 82, No. 6, pp. 1417-1422.

Grabić, M. L., Stupar, M., Vukojević, J., Maričić, I. and Bungur, N. (2013) Molds in museum environments: biodeterioration of art photographs and wooden sculptures, *Arch. Biol. Sci.*, Vol. 65, No. 3, pp. 955-962.

Hamed, S. A. and Mansour, M. M. A. (2018) Comparative study on micromorphological changes in wood due to soft-rot fungi and surface mold, *SC*, Vol. 4, No. 2, pp. 35-41.

Henriksson, M., Henriksson, G., Berglund, L. A. and Lindström, T. (2007) An environmentally friendly method for enzyme-assisted preparation of microfibrillated cellulose (MFC) nanofibers, *Eur. Polym. J.*, Vol. 43, No. 8, pp. 3434-3441.

Jahangeer, S., Khan, N., Jahangeer, S., Sohail, M., Shahzad, S., Ahmad, A. and Khan, Sh. A. (2005) Screening and characterization of fungal cellulases isolated from the native environmental source, *Pak. J. Bot.*, Vol. 37, No. 3, pp. 739-748.

Kavkler, K. and Demšar, A. (2012) Application of FTIR and Raman spectroscopy to qualitative analysis of structural changes in cellulosic fibres, *Tekstilec*, Vol. 55, No. 1, pp. 19-31.

Kavkler, K., Cimerman, N. G., Zalar, P. and Demšar A. (2015b) Deterioration of contemporary and artificially aged cotton by selected fungal species, *Polym. Degrad. Stabil.*, Vol. 113, pp. 1-9.

Kavkler, K., Gunde-Cimerman, N., Zalar, P. and Demšar, A. (2015a) Fungal contamination of textile objects preserved in Slovene museums and religious institutions, *Int. Biodeterior. Biodegradation*, Vol. 97, pp. 51-59.

Khan, G. M. A. and Alama, Md. Sh. (2012) Thermal characterization of chemically treated coconut husk fibre, *IJFTR* 37, 20-26.

Lee, K. and Inaba M. (2013) Moist heat accelerated aging test of naturally aged paper by suspension method, *Restaurator*, Vol. 34, No. 2, pp. 81-100.

Łojewska, J., Lubańska, A., Miśkowiec, P., Łojewski, T. and Proniewicz, L. M. (2006) FTIR in situ transmission studies on the kinetics of paper degradation via hydrolytic and oxidative reaction paths, *Appl. Phys. A*, Vol. 83, pp. 597-603.

Łojewska, J., Rabin, I., Pawcenis, D., Bagniuk, J., Aksamit-Koperska, M. A., Sitarz, M. Missori, M. and Krutzsch, M. (2017) Recognizing ancient papyri by a combination of spectroscopic, diffractional and chromatographic analytical tools, *Sci. Rep.* 7, on line at http://nbn-resolving.de/urn:nbn:de:kobv:b43-428704

Łojewski, T., Zięba, K., Knapik, A., Bagniuk, J., Lubańska, A. and Łojewska J. (2010) Evaluating paper degradation progress. Cross-linking between chromatographic, spectroscopic and chemical results, *Appl. Phys. A*, Vol. 100, pp. 809-821.

Palme A. (2015) *Characterization of cellulose in post-consumer cotton textiles*, PhD thesis, Chalmers University of Technology, Gothenburg, Sweden.

Pinzari, Fl., Pasquariello, Gr. and De Mico, A. (2006) Biodeterioration of paper: A SEM study of fungal spoilage reproduced under controlled conditions, *Macromol. Symp.*, Vol. 238, pp. 57-66.

Rao, S. (2009) *Enzymatic hydrolysis of cellulosic fiber*, Master thesis, Georgia Institute of Technology, Atlanta, USA.

Sterflinger, K. (2010) Fungi: Their role in deterioration of cultural heritage, *Fungal Biol. Rev.*, Vol. 24, No. 1-2, pp. 47-55.

Sterflinger, K. and Pinzari, Fl. (2012) The revenge of time: fungal deterioration of cultural heritage with particular reference to books, paper and parchment, *Environ. Microbiol.*, Vol. 14, No. 3, pp. 559-566.

Xu, C., Zhu, S., Xing, C., Li, D., Zhu, N. and Zhou, H. (2015) Isolation and properties of cellulose nanofibrils from coconut palm petioles by different mechanical process, *PLoS ONE*, Vol. 10, No. 4. https://doi.org/10.1371/journal.pone.0122123

Yang, H. (2011) *Investigation and characterization of oxidized cellulose and cellulose nanofiber films*, Master thesis, McGill University, Montreal, Quebec, Canada.

Yatagai, M. (1996) Dyeability of artificially aged cotton fibrics, *Text. Res. J.*, Vol. 66, No. 1, pp. 11-16.

APPENDIX

Appendix A. Schematic diagram of the research protocol

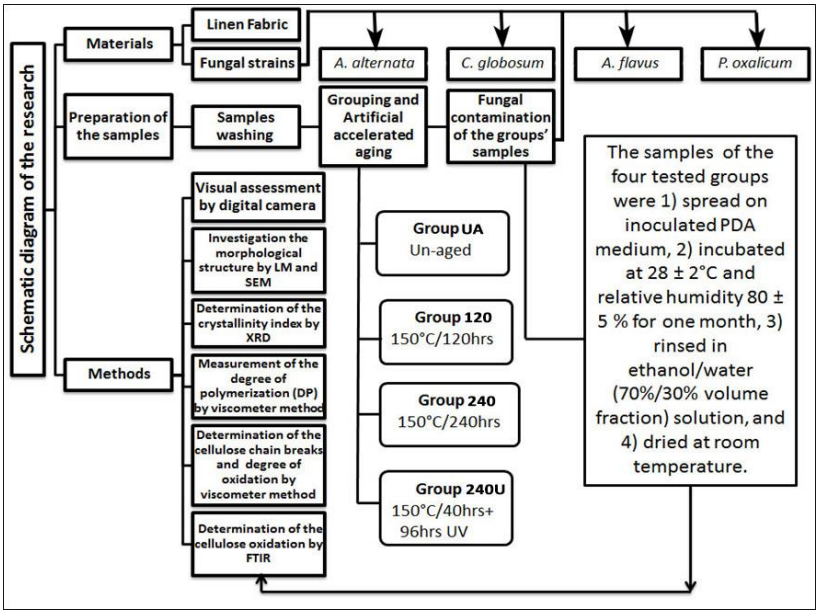

Appendix B. XRD diagrams of the samples from the four tested groups

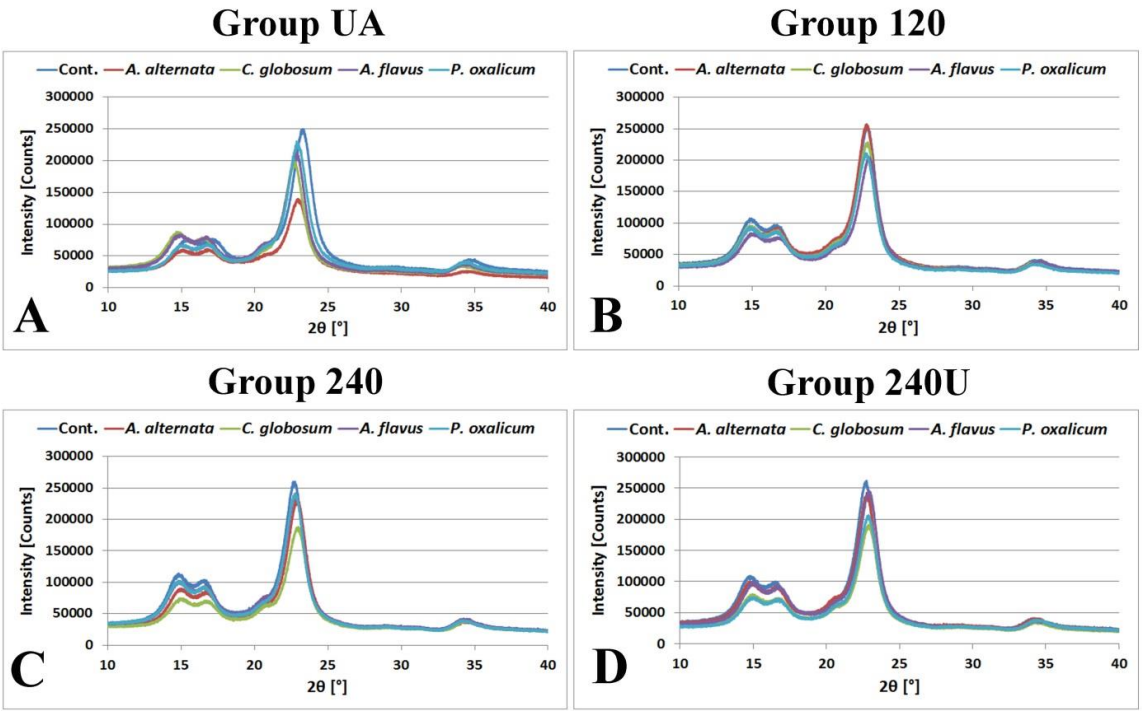

Appendix C. XRD data of the tested samples from the four groups

Group	Sample	Peak 002				Peak am				CrI	
		2θ[˚]		Intinsity (counts)		2θ[˚]		Intinsity (counts)		%	SD
		Value	SD	Value	SD	Value	SD	Value	SD		
UA	**Cont.**	23.2	0.115	197222	65859	18.7	0.024	41222	11809	78.5	2.04
	A.alternata	22.8	0.050	151472	20534	18.3	0.150	40944	4125	72.8	1.9
	C. globosum	22.5	0.190	214972	15066	18.2	0.084	47361	2246	77.9	1.1
	A. flavus	22.7	0.042	197722	11767	18.7	0.513	44000	3713	77.7	0.619
	P. oxalicum	22.8	0.045	190917	33638	18.5	0.327	41361	4930	78	2.16
120	**Cont.**	22.7	0.070	238945	17709	18.2	0.043	48444	4230	79.7	0.290
	A.alternata	22.70	0.027	213361	24545	18.2	0.110	46528	5358	78.1	1.90
	C. globosum	22.70	0.034	204805	31715	18.2	0.080	46389	7396	77.2	0.282
	A. flavus	22.80	0.028	207528	36203	18.3	0.108	44667	7432	78.4	0.970
	P. oxalicum	22.7	0.027	197500	13837	18.2	0.114	4511	4805	77.2	1.02
240	**Cont.**	22.6	0.012	242028	12471	18.3	0.214	49167	1651	79.7	0.80
	A.alternata	22.7	0.034	210028	47056	18.3	0.128	43417	7871	79	1.24
	C. globosum	22.8	0.060	173444	49598	18.2	0.050	39944	10015	76.7	1
	A. flavus	22.6	0.050	212889	29976	18.2	0.091	48945	6549	77	0.741
	P. oxalicum	22.6	0.025	232083	4574	18.3	0.094	47972	1024	79.3	0.125
240U	**Cont.**	22.6	0.008	238444	13365	18.2	0.070	47194	22128	80.2	0.754
	A.alternata	22.7	0.041	212306	26683	18.2	0.070	46084	5778	78.3	0.535
	C. globosum	22.8	0.021	184055	34226	18.6	0.271	40639	7059	77.8	0.250
	A. flavus	22.8	0.020	224555	28578	18.4	0.121	46139	6526	79.5	0.471
	P. oxalicum	22.8	0.064	176917	52354	18.3	0.030	38167	8827	77.8	2.01

Appendix D. FTIR-ATR spectra of the samples from the four tested groups: (A) Upper surface and (B) Lower surface.